Environ. Sci. Technol. **2007**, *41,* 4305−4310

A Model-Based Evaluation of Sorptive Reactivities of Hydrous Ferric Oxide and Hematite for U(VI)

JE-HUN JANG,* BRIAN A. DEMPSEY, AND WILLIAM D. BURGOS

Environmental Engineering, The Pennsylvania State University, 212 Sackett building, University Park, Pennsylvania 16802

The sorption of uranyl onto hydrous ferric oxide (HFO) or hematite was measured by discontinuously titrating the suspensions with uranyl at pH 5.9, 6.8, and 7.8 under $P_{CO_2} = 10^{-3.5}$atm (sorption isotherms). Batch reactors were used with equilibration times up to 48 days. Sorption of 1 μM uranyl onto HFO was also measured versus pH (sorption edge). A diffuse double layer surface complexation model was calibrated by invoking three sorption species that were consistent with spectroscopic evidence for predominance of bidentate complexes at neutral pH and uranyl−carbonato complexes: $>SOH:UO_2OH^{+1}$, $(>SO)_2:UO_2CO_3^{-2}$, and $(>SO)_2:(UO_2)_3(OH)_5^{-1}$. The model was consistent with previously published isotherm and edge data. The model successfully predicted sorption data onto hematite, only adjusting for different measured specific surface area. Success in application of the model to hematite indicates that the hydrated surface of hematite has similar sorptive reactivity as HFO.

Introduction

Hydrous ferric oxide (HFO) has a high sorption capacity for various contaminants. It occurs in natural waters as discrete particles or coatings on other minerals (*1*, *2*). HFO can transform into crystalline Fe (hydr)oxides (e.g., goethite, hematite, magnetite, etc.) (*3*, *4*). Based on bulk thermodynamic parameters, hematite (α-Fe_2O_3) is the most thermodynamically stable ferric oxide at ambient temperature and has been used to investigate the environmental reactions and significance of ferric oxide (*5*−*8*). HFO is the least stable and most soluble of the ferric (hydr)oxides. HFO forms preferentially when solutions are supersaturated, which is consistent with Ostwald's rule (*9*, *10*).

In both HFO and hematite, Fe^{+3} is octahedrally coordinated to surrounding ligands (O^{-2}, OH^-, or H_2O) (*3*, *4*). For HFO, random arrangement of the octahedra followed by polymerization (*11*) and hydration results in nondefinitive stoichiometry and diffused X-ray diffraction patterns, hence the crystallography and stoichiometry of HFO are unresolved (*3*, *12*, *13*). In hematite, Fe^{+3} is octahedrally coordinated to O^{-2} and Fe^{+3} occupies two thirds of the available octahedral sites (*14*).

Although hydroxyl ions and water molecules are not present in bulk hematite, the surface becomes hydrated. Tritium-exchange and discontinuous titrations of hematite indicate that the interfacial layers are goethite-like and extend 2.6 nm into the solid phase (*15*, *16*). Heat of immersion experiments show that the hydrated surface of hematite is multilayer and HFO-like (*17*, *18*). Ferrier (*19*) and Langmuir (*20*, *21*) demonstrated that hydrated goethite is stable relative to hydrated hematite in water at less than 80 °C, but Langmuir (*20*, *21*) noted that "the fact that pseudomorphs of goethite after hematite are unknown attests to the kinetic difficulty of rehydrating hematite." Despite the lack of evidence for conversion of bulk hematite to bulk goethite upon hydration, the conversion of hematite (0001) surface to FeOOH or $Fe(OH)_3$ has been detected using X-ray photoemission spectroscopy (*22*).

A few investigations have compared the sorptive reactivities of various Fe(III) (hydr)oxides with respect to one probing sorbate, and these studies implied that the sorptive reactivities of various ferric (hydr)oxides could be similar. Dixit and Hering (*23*) investigated the sorption of arsenic onto goethite, HFO, and magnetite; three solids showed similar affinities for As(III) and similar surface site densities for both As(V) and As(III). Charlet and Manceau (*24*) used X-ray absorption fine-structure (EXAFS) spectroscopy and found that Cr(III) sorbs onto goethite and HFO by inner-sphere poly-Cr complexes. Spadini et al. (*12*) showed that Cd^{2+} sorbed on HFO and goethite showed similar first- and second-nearest Fe(III) nearest-neighbor distances (R_1 and R_2, respectively). Another EXAFS study revealed that Pb(II) forms identical mononuclear bidentate complexes to edges of the surface octahedra on both goethite and hematite (*25*).

U(VI) exhibits a rapid increase in sorption on HFO from pH 4 to 6, followed by a sharp decrease when pH exceeds 8 in the presence of carbonate (*5*, *26*−*29*). Hsi and Langmuir (*26*) measured U(VI) sorption onto HFO, goethite, and hematite with up to 0.01 M $NaHCO_3$ using different suites of constants for the three systems. Based on crystallographic considerations, Hsi and Langmuir (*26*) predicted that a bidentate surface complex of $(UO_2)_3(OH)_5^+$ was the predominant surface species. The model was inaccurate for carbonate-containing solutions. Ho and Miller (*5*) attributed the decrease in sorption with higher pH to the decline in concentration of a proposed $(UO_2)_2CO_3(OH)_3^-$ species (*30*). Bargar et al. (*6*, *7*) described EXAFS (pH 6.5) and electrophoretic mobility data supporting the formation of bidentate uranyl−carbonato complexes on hematite. Waite et al. (*28*) measured U(VI) sorption onto HFO with P_{CO_2}=$10^{-3.5}$atm as a function of $U(VI)_T$, ionic strength, and $Fe(III)_T$. Their model was based on wet sorption studies over a range of conditions and EXAFS samples that were prepared at pH 5 and 5.5. The model included four surface complexation constants, i.e., strong and weak sites for two bidentate complexes $(>FeO_2)UO_2$ and $(>FeO_2)UO_2CO_3^{2-}$. Using the Waite et al. (*28*) data and constants, we obtained best fit for their adsorption edge and surface speciation (their Figure 12b) by assuming mononuclear bidentate surface sites, i.e., the extent of adsorption was first order with respect to the concentration of surface sites, consistent with their model structure shown in their Figure 10. None of these papers investigated the hypothesis that different ferric oxides might have similar sorptive reactivity.

The objective of this study was to compare the sorption of uranyl (UO_2^{2+}) onto two Fe(III) (hydr)oxides, HFO (amorphous solid) or hematite (α-Fe_2O_3, crystalline solid) in order to test the hypothesis that sorptive reactivities of the two surfaces are similar. The surfaces were discontinuously titrated with UO_2^{2+} at pH 5.9, 6.8, and 7.8 under $P_{CO_2} = 10^{-3.5}$atm using batch reactors (sorption isotherm experiments), with reaction time up to 48 days. The sorption of 1

* Corresponding author phone: (814)441-1527; fax: (814)863-7304; e-mail: jhjang2004@gmail.com.

10.1021/es070068f CCC: $37.00
Published on Web 05/18/2007

μM uranyl onto HFO versus pH was also measured (sorption edge experiments).

Materials and Methods

Solutions were prepared using deionized distilled (DI) water (~18MΩ·cm). Chemicals were reagent grade or better. Containers were acid-washed (10% HNO_3) and rinsed with DI water. U(VI) stocks (uranyl acetate) were prepared in 0.01 or 0.1 M HNO_3. Chloride was not used due to interference with kinetic phosphorescence analysis (KPA-11, ChemChek, Inc., Richland, WA) for U(VI). KPA protocols were previously described (*31*−*33*).

The synthesis and cleaning of hydrous ferric oxide (HFO) and hematite were previously described (*31*). The pH of a $FeCl_3$ solution was adjusted with 1.0 or 0.1 M NaOH to pH ~7 for synthesis of HFO. Hematite was prepared by thermally forced hydrolysis at 100 °C for 5 days (*34*, *35*). Suspensions were always in contact with water, i.e., never dried. The procedure for HFO synthesis (*36*) results in N_2-BET surface area of 182 m^2/g. Other reports of N_2-BET surface area for HFO range from 159−234 m^2/g (*37*). N_2-BET surface area of hematite was 38 m^2/g (Material Characterization Laboratory, Pennsylvania State University), one-fifth the specific surface area of HFO. HFO primary particles are ~2 nm in diameter (*38*); hematite particles were 100 nm diameter by transmission electron microscopy.

HFO suspensions were aged 4 days prior to the addition of U(VI). In other studies HFO has been aged 4 h (*26*), 24 h (*27*), or 113 h (*28*) prior to the addition of U(VI). Total Fe(III) in HFO and hematite stock suspensions was analyzed using 1,10-phenanthroline after reduction to Fe(II) (*39*). Mössbauer spectroscopy (*40*, *41*) was used to analyze 4-day-aged HFO and HFO aged with and without uranyl for an additional 48 days.

For sorption isotherm experiments, the pH of DI water (90% of the desired final volume) was adjusted more than seven times over 2 days to 5.9, 6.8, or 7.8 while bubbling with water-saturated air ($P_{CO_2} = 10^{-3.5}$atm). HFO or hematite was added to provide 0.1 mM Fe(III) in the final suspension (100 mL total volume), ionic strength ($NaNO_3$) was 0.01, and suspensions were equilibrated with air for 1 more day. U(VI) stock was added, pH was adjusted frequently, and the volume of the suspension was monitored by analytical balance. Sorption on HFO was measured after 1, 3, 6, 12, 25, and 48 days; there was a 33% decrease in average partition coefficient (ratio of sorbed to dissolved U) on HFO for 12−48 days compared to 1−6 days. Sorption of U(VI) onto hematite was measured at 0.01, 1, 3, 6, 12, 25, and 48 days; the average partition coefficient increased by 0.1% on hematite for 12−48 days compared to 0.01−6 days. Accordingly we constructed and calibrated our sorption model using only the HFO data for 1−6 days. Other investigators have used 4 h to 2 days equilibration for sorption of U(VI) on HFO (*26*−*28*).

Dissolved U(VI) was determined as concentration in the filtrate (0.2 μm) divided by permeation coefficients, i.e., the ratio of filtered U(VI) to total dissolved U(VI) in check solutions at each pH. Total U(VI) was determined after extraction of the suspension in 0.5 M HNO_3 for 24 h. Sorbed U(VI) was the difference between total and dissolved U(VI).

Sorption edge experiments (uranyl sorption vs pH) were conducted in 250 mL plastic beakers using 1 μM U(VI), 1 mM Fe(III) as HFO, and $I = 0.1$ by titrating the suspension (initial pH < 3) with 1.00 M NaOH. Sampling for total and dissolved U(VI) and pH measurement were performed 5 min after each addition of titrant. The reactor was gently stirred; Total inorganic carbon (TIC) ranged from 10 μM at pH 3 to 60 μM at the end of the titration.

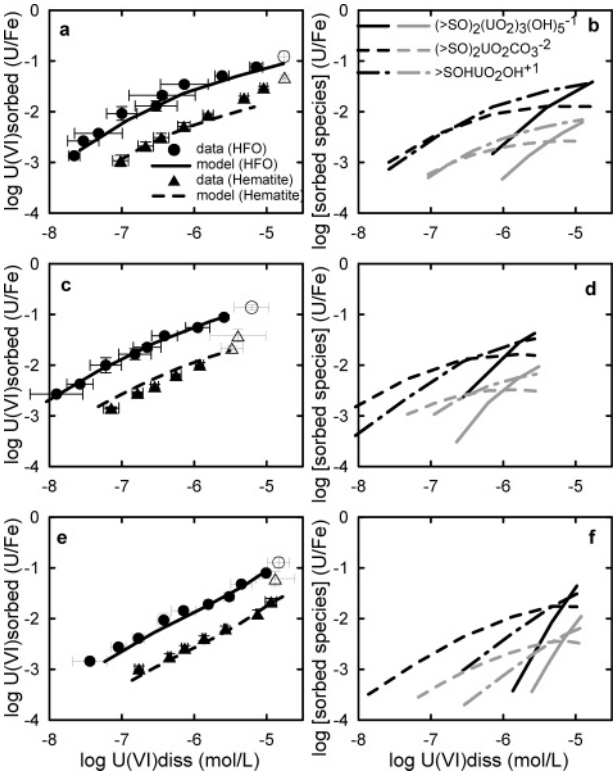

FIGURE 1. Sorption of U(VI) onto Hydrous Ferric Oxide (circles) and hematite (triangles): (a, b) pH 5.9, (c, d) pH 6.8, and (e, f) pH 7.8. Open symbols indicate where schoepite precipitates (*31*, *44*). They were excluded from model calibration. Curves in (a, c, e) show predictions of sorption. Curves in (b, d, f) show predicted concentrations of U(VI) in the surface species; black lines for HFO and gray lines for hematite.

Results and Discussion

Calibration of a Surface Complexation Model Using U(VI) Sorption onto HFO. Symbols in Figure 1(a, c, e) represent averages and standard deviations for sorption of U(VI) onto HFO and hematite. A surface complexation model was constructed and calibrated using only the HFO data. Dzombak and Morel proposed two-sites (0.200 and 0.005 site/Fe for weak and strong site) for a variety of sorbates with HFO (*1*), but we obtained good fits using a one-site model (0.205 site/Fe, or 2.3 sites/nm^2). Wazne et al. (*29*) also reported that a single-site model was adequate for sorption of U(VI) on HFO. Bargar et al. (*7*) and Waite et al. (*28*) invoked higher surface site densities, 19 and 10 sites/nm^2, respectively. Table 1 includes the reactions that were calibrated in this study. Surface acidity constants (vii, viii) were consistent with previously reported values (*1*). Constants for reactions (ix, x) were from ref *42*. Only three new constants (xi−xiii) were estimated from the HFO data, by minimizing residual errors (differences between experimental and predicted sorption isotherms) at each pH using Visual MINTEQ (*43*) for computations. The use of same model for hematite experiment is discussed in section below.

We used Langmuir's formation constants in this paper (i−vi, Table 1, (*31*, *44*)), resulting in UO_2OH^+, $(UO_2)_3(OH)_5^+$, and $UO_2CO_3^0$ as the most abundant soluble species over the pH range of this study (Figure 2). We previously reported that, for similar experimental conditions, the solubility of schoepite versus pH was best fit using the suite of formation constants in Langmuir (*44*). Others have proposed $(UO_2)_2(OH)_3CO_3^-$ (*30*, *45*, *46*) or $UO_2(OH)_2^\circ$ (*47*) as major dissolved species. The most accurate work identifying a formation constant for $(UO_2)_2(OH)_3CO_3^-$ was performed at $P_{CO_2} \geq 0.3$ atm and pH < 5.7 (*45*), i.e., conditions very different

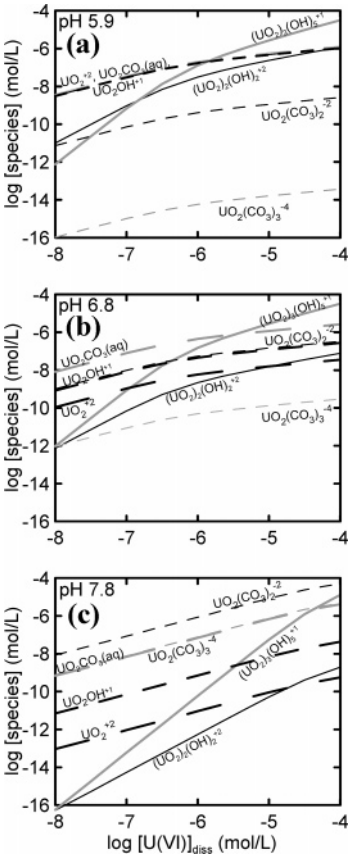

FIGURE 2. Predicted concentrations of aqueous species as a function of total [U(VI)$_{diss}$] using reactions in Table 1. UO_2OH^{+1}, $UO_2CO_3^0$, and $(UO_2)_3(OH)_5^{+1}$ were selected as sorbate species.

TABLE 1. Aqueous Speciation (*31*, *44*) and Surface Complexation Reactions for Uranyl

aqueous speciation	log *K*
$UO_2^{+2} + H_2O \leftrightarrow UO_2OH^+ + H^+$	−5.78 (i)
$2UO_2^{+2} + 2H_2O \leftrightarrow (UO_2)_2(OH)_2^{+2} + 2H^+$	−5.62 (ii)
$3UO_2^{+2} + 5H_2O \leftrightarrow (UO_2)_3(OH)_5^+ + 5H^+$	−15.63 (iii)
$UO_2^{+2} + CO_3^{-2} \leftrightarrow UO_2(CO_3)^\circ$	10.06 (iv)
$UO_2^{+2} + 2CO_3^{-2} \leftrightarrow UO_2(CO_3)_2^{-2}$	16.98 (v)
$UO_2^{+2} + 3CO_3^{-2} \leftrightarrow UO_2(CO_3)_3^{-4}$	21.40 (vi)
surface complexation	
$>SOH_2^+ \leftrightarrow >SOH^0 + H^+$	−7.29 (vii)
$>SOH^0 \leftrightarrow >SO^- + H^+$	−8.93 (viii)
$>SOH^0 + CO_3^{-2} + 2H^+ \leftrightarrow >SOH{:}\ CO_3H_2^0$	19.56 (ix)
$>SOH^0 + CO_3^{-2} + H^+ \leftrightarrow >SOH{:}\ CO_3H^-$	10.76 (x)
$>SOH^0 + UO_2^{+2} + H_2O \leftrightarrow >SOH{:}\ UO_2OH^{+1} + H^+$	*2.0*[a] (xi)
$2>SOH^0 + 3UO_2^{+2} + 5H_2O \leftrightarrow (>SO)_2{:}\ (UO_2)_3(OH)_5^{-1} + 7H^+$	*−24.3* (xii)
$2>SOH^0 + UO_2^{+2} + CO_3^{-2} \leftrightarrow (>SO)_2{:}\ UO_2CO_3^{-2} + 2H^+$	*0.5* (xiii)

[a] Modeling parameters are in *italic*.

from those employed in our work. The constant for $UO_2(OH)_2^\circ$ is still speculative and has been reported as $\log\beta_2 < -10.3$ in ref *47*. Guillaumont et al. (*48*) provided updates for (*47*) and $\log\beta_2 = -12.15$ in their work (*48*). If additional species or different formation constants were used, then values for the surface complexation constants would also be different (*49*).

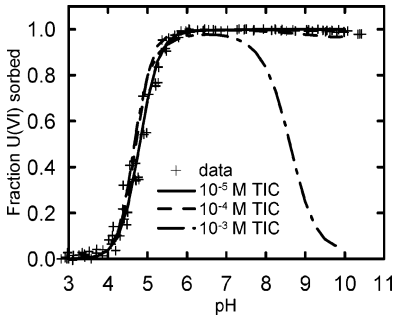

FIGURE 3. Sorption of uranyl as a function of pH (sorption edge) measured in this study: $U(VI)_{total} = 1\ \mu M$, $Fe(III)_{total} = 1$ mM (as HFO), total inorganic carbon (TIC) = 10∼60 μM, and $I = 0.1$. Curves represent predictions using the reactions in Table 1.

The best fit for the HFO sorption isotherms was obtained by invoking three surface complexes: $>SOH{:}UO_2OH^{+1}$, $(>SO)_2{:}(UO_2)_3(OH)_5^{-1}$, and $(>SO)_2{:}UO_2CO_3^{-2}$. Mono-hydroxy monomers are typically invoked as a major sorbed species, due to decreased solvation energy compared to the divalent metals (*50*). Sorption of $UO_2CO_3^0$ and formation of bidentate surface complexes were based on EXAFS spectroscopy of uranyl sorbed onto hematite in the presence of carbonate (*6*, *7*, *28*). The inflection in sorption for high dissolved U(VI) at pH 7.8 (Figure 1e) required $(UO_2)_3(OH)_5^+$ as a sorbate, as reported in other studies (*51*, *52*). We modeled $>SOH{:}UO_2OH^{+1}$ as first order with respect to the concentration of surface sites, i.e., the same stoichiometry for surface sites that was invoked by Waite et al. (*21*) for mononuclear bidentate adsorption of UO_2^{+2}. We modeled $(>SO)_2{:}(UO_2)_3(OH)_5^{-1}$ and $(>SO)_2{:}UO_2CO_3^{-2}$ as second-order reactions with respect to surface sites. Results from the sorption edge experiments of this study are shown by the symbols in Figure 3. Predicted sorption are shown by the lines, based on reactions in Table 1. Model predictions shown are for 10, 100, and 1000 μM TIC (total inorganic carbon).

Validation of Our Model Using Published U(VI) Sorption Data. The model was successfully applied to previously published sorption isotherm and edge data; Morrison et al. (*27*) ran experiments at pH 7.0 with various TIC using HFO. Their isotherms for 0 and 1.9 mM TIC (initial values) are shown by the data in Figure 4a. Our model fit the Morrison data for zero TIC, but under-predicted sorption using their reported TIC of ∼1.7 mM (10% loss of TIC into the headspace); we obtained a better fit using TIC of 0.95 mM, consistent with greater volatilization of CO_2 than was reported in their paper (*27*). U(VI) sorption onto goethite ($I = 0.001$ to 0.1) (*53*) was also well predicted using our model (Figure 4b). Waite et al. (*28*) used the same U(VI) and Fe(III) concentrations as in our experiment but at different ionic strength. Their data and our predictions are shown in Figure 4c.

These results demonstrate that our simple model for speciation and sorption of U(VI) onto Fe(III) (hydr)oxides accurately described U(VI) speciation over a wide range of pH, TIC, ionic strength, mineralogy, and sorbate/sorbent ratio. We do not exclude that other suites of surface reactions could describe the data equally well. Although it is impossible to uniquely identify the predominant surface reactions solely based on the goodness of fit (*26*, *49*), our model is consistent with published EXAFS results (*6*, *7*, *28*) and with electrophoretic data, especially reversal of charge with increasing U(VI) at pH > 6.5 (*7*).

Application of the Model to Hematite Experiments. We then used our model to test the hypothesis that hematite may have sorptive reactivity similar to HFO. Surface complexation constants that were calibrated using the HFO data (Table 1) were used to predict sorption of U(VI) onto hematite. The only change in model parameters was for lower measured

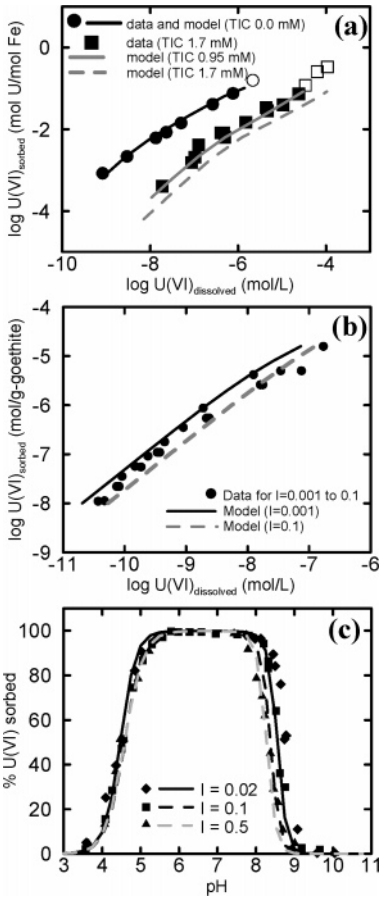

FIGURE 4. Symbols represent published sorption isotherm data on (a) HFO from (*27*) and (b) goethite from (*53*). Open symbols in (a) represent supersaturated conditions relative to schoepite (log*K_{sp} = 5.39) determined by reactions in Table 1. Aqueous and surface reactions of this study are listed in Table 1 (*31*, *44*). (a) and (b) are for pH 7.0. (c) HFO data from (*28*): $U(VI)_{total}$=1 μM, $Fe(III)_{total}$=1 mM (as HFO), $P_{CO_2}=10^{-3.5}$atm, and I = 0.02, 0.1, or 0.5. Lines in (a, b, c) are predictions using the reactions in Table 1.

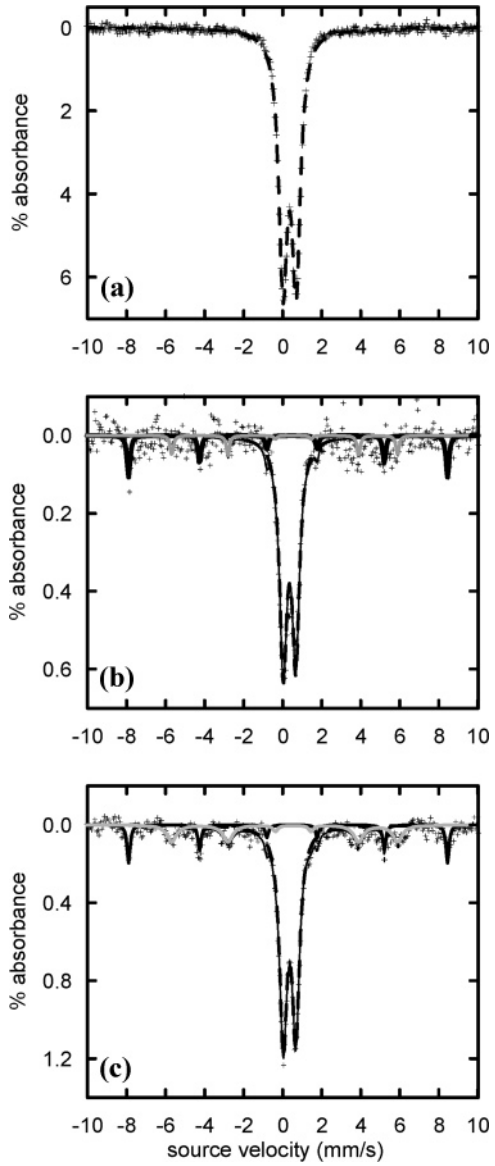

FIGURE 5. Mössbauer spectroscopy of hydrous ferric oxide. (a) HFO 4 days after synthesis, (b) HFO aged in water without uranyl for 48 days, and (c) HFO aged with uranyl for 48 days. HFO evolved into a mixture of HFO (largest peaks in the middle in (a, b, c), thick black dashed line), hematite (6 peaks with solid black lines in (b, c)), and goethite (6 peaks with solid gray lines in (b, c)). The ratios of HFO:hematite:goethite were 80:13:7 in (b) and 72:11:17 in (c), indicating that uranyl enhanced the transformation of HFO into goethite.

specific surface area of hematite. Predicted sorption of U(VI) onto hematite and surface speciation are shown in Figure 1. The good fit between predicted and experimental sorption for hematite is consistent with the stated hypothesis.

Implication for Environmental Iron Chemistry. Transformations among ferric oxides are well-documented and can be accelerated by redox reactions associated with metal sorption onto HFO (*40*, *54*, *55*). Evidence for transformations is based on bulk phase analyses rather than interfacial analyses, but transformation can result in decreased specific surface area (*37*). We reported above that sorption onto HFO decreased with longer reaction times, consistent with ref *56* and consistent with our Mössbauer spectroscopy, demonstrating some conversion of HFO into goethite and hematite at 48 days of aging. Aging in the presence of uranyl resulted in additional conversion to goethite (Figure 5). Goethite forms via incongruent dissolution and reprecipitation while hematite is formed through internal dehydration and rearrangement of HFO (*57*, *58*).

The conversion to more stable phases is consistent with the literature that was cited earlier in this paper (*15*, *16*, *20*–*22*), i.e., transformation to a more stable bulk phase (hematite or goethite) occurs in zones that are separated from the solid–water interface while a more reactive hydrated phase remains stable at the solid–water interface. The observation that identical complexation constants could be used to describe sorption of U(VI) onto HFO and hematite is consistent with the hypothesis that the hydrated surface of hematite exhibits similar reactivity as HFO, as proposed by DeBruyn and co-workers where they reported a time-dependent increase in surface protonation on hematite, resulting in a total surface charge that exceeded the capacity of a monolayer (*15*, *16*). These results are also consistent with thermodynamic evidence (*19*–*22*) indicating stability of hydrated goethite compared to hydrated hematite.

Acknowledgments

This research was supported by the Office of Science (BER), U.S. Department of Energy, grant no. DE-FG02-04ER63914 and by the National Science Foundation under grant no. BES-0523196.

Literature Cited

(1) Dzombak, D. A.; Morel, F. M. M. *Surface Complexation Modeling: Hydrous Ferric Oxide*; John Wiley & Sons: New York, 1990.

(2) Jenne, E. A. Controls on Mn, Fe, Co, Ni, Cu, and Zn concentrations in soils and water: the significant role of hydrous Mn and Fe oxides. In *Trace Inorganics in Water*; Baker, R. A., Ed.; American Chemical Society: Washington, DC, 1968; pp 337−387.

(3) Drits, V. A.; Sakharov, B. A.; Salyn, A. L.; Manceau, A. Structural model for ferrihydrite. *Clay Miner.* **1993**, *28*, 185−207.

(4) Manceau, A.; Gates, W. P. Surface structural model for ferrihydrite. *Clays Clay Miner.* **1997**, *45*, 448−460.

(5) Ho, C. H.; Miller, N. H. Adsorption of uranyl species from bicarbonate solution onto hematite particles. *J. Colloid Interface Sci.* **1986**, *110*, 165−171.

(6) Bargar, J. R.; Reitmeyer, R.; Davis, J. A. Spectroscopic confirmation of uranium(VI)-carbonato adsorption complexes on hematite. *Environ. Sci. Technol.* **1999**, *33*, 2481−2484.

(7) Bargar, J. R.; Reitmeyer, R.; Lenhart, J. J.; Davis, J. A. Characterization of U(VI)-carbonato ternary complexes on hematite: EXAFS and electrophoretic mobility measurements. *Geochim. Cosmochim. Acta.* **2000**, *64*, 2737−2749.

(8) Lenhart, J. J.; Honeyman, B. D. Uranium(VI) sorption to hematite in the presence of humic acid. *Geochim. Cosmochim. Acta.* **1999**, *63*, 2891−2901.

(9) Morse, J. W.; Casey, W. H. Ostwald processes and mineral paragenesis in sediments. *Am. J. Sci.* **1988**, *288*, 537−560.

(10) Steefel, C. I.; van Cappellen, P. A new kinetic approach to modeling water-rock interaction: The role of nucleation, precursors, and Ostwald ripening. *Geochim. Cosmochim. Acta.* **1990**, *54*, 2657−2677.

(11) Davis, J. A.; Kent, D. B. Surface complexation modeling in aqueous geochemistry. In *Mineral-Water Interface Geochemistry*; Hochella, M. F., Jr.; White, A. F., Eds.; Mineralogical Society of America: Chantilly, VA, 1990; Vol. 23, pp 177−260.

(12) Spadini, L.; Manceau, A.; Schindler, P. W.; Charlet, L. Structure and stability of Cd^{2+} surface complexes on ferric oxides. *J. Colloid Interface Sci.* **1994**, *168*, 73−86.

(13) Cardile, C. M. Tetrahedral Fe^{3+} in ferrihydrite: ^{57}Fe Mössbauer spectroscopic evidence. *Clays Clay Miner.* **1988**, *36*, 537−539.

(14) Cornell, R. M.; Schwertmann, U. *The Iron Oxides: Structure, Properties, Reactions, Occurrence and Uses*; VCH Publisher: New York, 1996.

(15) Onoda, G. Y., Jr.; de Bruyn, P. L. Proton adsorption at the ferric oxide/aqueous solution interface. I. A kinetic study of adsorption. *Surf. Sci.* **1966**, *4*, 48−63.

(16) Berube, Y. G.; Onoda, G. Y., Jr.; de Bruyn, P. L. Proton adsorption at the ferric oxide/aqueous solution interface. II. Analysis of kinetic data. *Surf. Sci.* **1967**, *8*, 448−461.

(17) Zettlemoyer, A. C.; McCafferty, E. The heat of immersion on α-Fe_2O_3 in water. *Z. Phys. Chem.* 1969, *64*, 41−48.

(18) McCafferty, E.; Zettlemoyer, A. C. Adsorption of water vapour on α-Fe_2O_3. *Discuss. Faraday Soc.* **1971**, *52*, 239−254.

(19) Ferrier, A. Influence de l'etat de division de la goethite et de l'oxyde ferrique sur leurs chaleurs de reaction. *Rev. Chim. Miner.* **1966**, *3*, 587−615.

(20) Langmuir, D. Particle size effect on the reaction goethite = hematite + water. *Am. J. Sci.* **1971**, *271*, 147−156.

(21) Langmuir, D. Correction: Particle size effect on the reaction goethite = hematite + water. *Am. J. Sci.* **1972**, *272*, 972.

(22) Liu, P.; Kendelewicz, T.; Brown, G. E., Jr.; Nelson, E. J.; Chambers, S. A. Reaction of water vapor with α-Al_2O_3(0001) and α-Fe_2O_3-(0001) surfaces: synchrotron X-ray photoemission studies and thermodynamic calculations. *Surf. Sci.* **1998**, *417*, 53−65.

(23) Dixit, S.; Hering, J. G. Comparison of arsenic(V) and arsenic(III) sorption onto iron oxide minerals: Implications for arsenic mobility. *Environ. Sci. Technol.* **2003**, *37*, 4182−4189.

(24) Charlet, L.; Manceau, A. A. X-ray absorption spectroscopic study of the sorption of Cr(III) at the oxide-water interface. *J. Colloid Interface Sci.* **1992**, *148*, 443−458.

(25) Bargar, J. R.; Brown, J.; G. E.; Parks, G. A. Surface complexation of Pb(II) at oxide-water interfaces: II. XAFS and bond-valence determination of mononuclear Pb(II) sorption products and surface functional groups on iron oxides. *Geochim. Cosmochim. Acta* **1997**, *61*, 2639−2652.

(26) Hsi, C.-K. D.; Langmuir, D. Adsorption of uranyl onto ferric oxyhydroxides: Application of the surface complexation site-binding model. *Geochim. Cosmochim. Acta.* **1985**, *49*, 1931−1941.

(27) Morrison, S. J.; Spangler, R. R.; Tripathi, V. S. Adsorption of uranium(VI) on amorphous ferric oxyhydroxide at high concentrations of dissolved carbon(IV) and sulfur(VI). *J. Contam. Hydrol.* **1995**, *17*, 333−346.

(28) Waite, T. D.; Davis, J. A.; Payne, T. E.; Waychunas, G. A.; Xu, N. Uranium(VI) adsorption to ferrihydrite: Application of a surface complexation model. *Geochim. Cosmochim. Acta.* **1994**, *58*, 5465−5478.

(29) Wazne, M.; Korfiatis, G. P.; Meng, X. Carbonate effects on hexavalent uranium adsorption by iron oxyhydroxide. *Environ. Sci. Technol.* **2003**, *37*, 3619−3624.

(30) Maya, L. Hydrolysis and carbonate complexation of dioxouranium(VI) in the neutral-pH range at 25 °C. *Inorg. Chem.* **1982**, *21*, 2895−2898.

(31) Jang, J.-H.; Dempsey, B. A.; Burgos, W. D. Solubility of schoepite: Comparison and selection of complexation constants for U(VI). *Water Res.* **2006**, *40*, 2738−2746.

(32) Sowder, A. G.; Clark, S. B.; Fjeld, R. A. The effect of sample matrix quenching on the measurement of trace uranium concentrations in aqueous solutions using kinetic phosphorimetry. *J. Radioanal. Nucl. Chem.* **1998**, *234*, 257−260.

(33) Brina, R.; Miller, A. G. Direct detection of trace levels of uranium by laser-induced kinetic phosphorimetry. *Anal. Chem.* **1992**, *64*, 1413−1418.

(34) Raming, T. P.; Winnubst, A. J. A.; van Kats, C. M.; Philipse, A. P. The synthesis and magnetic properties of nanosized hematite (α-Fe_2O_3) particles. *J. Colloid Interface Sci.* **2002**, *249*, 346−350.

(35) Sugimoto, T.; Muramatsu, A. Formation mechanism of monodispersed α-Fe_2O_3 particles in dilute $FeCl_3$ solutions. *J. Colloid Interface Sci.* **1996**, *184*, 626−638.

(36) Davis, J. A.; Leckie, J. O. Surface ionization and complexation at the oxide/water interface II. Surface properties of amorphous iron oxyhydroxide and adsorption of metal ions. *J. Colloid Interface Sci.* **1978**, *67*, 90−107.

(37) Crosby, S. A.; Glasson, D. R.; Cuttler, A. H.; Butler, I.; Turner, D. R.; Whitfield, M.; Millward, G. E. Surface areas and porosities of Fe(III)- and Fe(II)-derived oxyhydroxides. *Environ. Sci. Technol.* **1983**, *17*, 709−713.

(38) Murphy, P. J.; Posner, A. M.; Quirk, J. P. Characterization of partially neutralized ferric nitrate solutions. *J. Colloid Interface Sci.* **1976**, *56*, 270−283.

(39) APHA *Standard Methods for the Examination of Water and Wastewater*, 18th ed.; American Public Health Association: Washington, DC, 1992.

(40) Jang, J.-H.; Dempsey, B. A.; Catchen, G. L.; Burgos, W. D. Effects of Zn(II), Cu(II), Mn(II), Fe(II), NO_3^-, or SO_4^{2-} at pH 6.5 and 8.5 on transformations of hydrous ferric oxide (HFO) as evidenced by Mössbauer spectroscopy. *Colloids Surf., A.* **2003**, *221*, 55−68.

(41) Hawthorne, F. C. Mössbauer Spectroscopy. In *Spectroscopic methods in mineralogy and geochemistry*; Hawthorne, F. C., Ed.; Mineralogical Society of America, 1988; Vol. 18.

(42) Zachara, J. M.; Girvin, D. C.; Schmidt, R. L.; Resch, C. T. Chromate adsorption on amorphous iron oxyhydroxide in the presence of major groundwater ions. *Environ. Sci. Technol.* **1987**, *21*, 589−594.

(43) Gustafsson, J. P. Visual MINTEQ 2.50. 2006.

(44) Langmuir, D. Uranium solution-mineral equilibria at low temperatures with applications to sedimentary ore deposits. *Geochim. Cosmochim. Acta.* **1978**, *42*, 547−569.

(45) Grenthe, I.; Lagernan, B. Studies on metal carbonate equilibria. 22. A coulometric study of the uranium(VI)-carbonate system, the composition of the mixed hydroxide carbonate species. *Acta. Chem. Scand.* **1991**, *45*, 122−128.

(46) Szabó, Z.; Moll, H.; Grenthe, I. Structure and dynamics in the complex ion $(UO_2)_2(CO_3)(OH)_3^-$. *J. Chem. Soc. Dalton Trans.* **2000**, *18*, 3158−3161.

(47) Grenthe, I.; Fuger, J.; Koning, R. J. M.; Lemire, R. J.; Muller, A. B.; Nguyen-Trung, C.; Wanner, H. *Chemical Thermodynamics of Uranium*; North-Holland: Amsterdam, 1992; Vol. 1.

(48) Guillaumont, R.; Fanghänel, T.; Fuger, J.; Grenthe, I.; Neck, V.; Palmer, D. A.; Rand, M. H. *Update on the chemical thermodynamics of uranium, neptunium, plutonium, americium and technetium*; Elsevier: Amsterdam, 2003; Vol. 5.

(49) Westall, J.; Hohl, H. A comparison of electrostatic models for the oxide/solution interface. *Adv. Colloid Interface Sci.* **1980**, *12*, 265−294.

(50) James, R. O.; Healy, T. W. Adsorption of hydrolyzable metal ions at the oxide-water interface. III. A thermodynamic model of adsorption. *J. Colloid Interface Sci.* **1972**, *40*, 65−81.

(51) Katz, L. E.; Hayes, K. F. Surface complexation modeling. II. Strategy for modeling polymer and precipitation reactions at high surface coverage. *J. Colloid Interface Sci.* **1995**, *170*, 491−501.

(52) Ford, R. G.; Scheinost, A. C.; Sparks, D. L. Frontiers in metal sorption/precipitation mechanisms on soil mineral surfaces. *Adv. Agron.* **2001**, *74*, 41−62.

(53) Missana, T.; Garcia-Gutierrez, M.; Maffiotte, C. Experimental and modeling study of the uranium (VI) sorption on goethite. *J. Colloid Interface Sci.* **2003**, *260*, 291−301.

(54) Cornell, R. M. The influence of some divalent cations on the transformation of ferrihydrite to more crystalline products. *Clay Miner.* **1988**, *23*, 329−332.

(55) Pedersen, H. D.; Postma, D.; Jakobsen, R.; Larsen, O. Fast transformation of iron oxyhydroxides by the catalytic action of aqueous Fe(II). *Geochim. Cosmochim. Acta.* **2005**, *69*, 3967−3977.

(56) Ainsworth, C. C.; Pilon, J. L.; Gassman, P. L.; van der Sluys, W. G. Cobalt, cadmium, and lead sorption to hydrous iron oxide: residence time effect. *Soil Sci. Soc. Am. J.* **1994**, *58*, 1615−1623.

(57) Schwertmann, U.; Friedl, J.; Stanjek, H. From Fe(III) ions to ferrihydrite and then to hematite. *J. Colloid Interface Sci.* **1999**, *209*, 215−223.

(58) Schwertmann, U.; Murad, E. Effect of pH on the transformation of goethite and hematite from ferrihydrite. *Clays Clay Miner.* **1983**, *31*, 277−284.

Received for review January 10, 2007. Revised manuscript received April 13, 2007. Accepted April 16, 2007.

ES070068F